ELSEVIER

Journal of Organometallic Chemistry 565 (1998) 201–210

Journal of Organo metallic Chemistry

Organolanthanoids XXIII[1] complexes of tris(cyclopentadienyl)lanthanoids with tertiary phosphine oxides and the X-ray crystal structures of $[YbCp_3(OPPh_3)]$ and $[NdCp_3(OPBu^n_3)]$[2]

Glen B. Deacon *, Gary D. Fallon, Craig M. Forsyth, Bryan M. Gatehouse, Peter C. Junk, Anna Philosof, Paul A. White

Chemistry Department, Monash University, Clayton, Victoria 3168, Australia

Received 12 December 1997

Abstract

Treatment of $[LnCp_3(THF)]$ (Ln = La, Nd, Sm, or Yb) (Cp, cyclopentadienyl and THF, tetrahydrofuran) and $[Nd(MeCp)_3(THF)]$ (MeCp, methylcyclopentadienyl) with OPR_3 (R = Ph, *o*-tolyl, Bu^n) in either THF or DME (DME, 1,2-dimethoxyethane) gave the complexes $[LnCp_3(OPPh_3)]$ (Ln = La, Nd, Sm and Yb), $[Nd(MeCp)_3(OPPh_3)]$, $[SmCp_3(OP(o\text{-tolyl})_3)]$, $[Nd(MeCp)_3(OP(o\text{-tolyl})_3)]$, and $[LnCp_3(OPBu^n_3)]$ (Ln = La, Nd). An attempt to react $[GdCp_3(THF)]$ with $OPPh_3$ in either THF or DME crystallised unsolvated $GdCp_3$, whilst a mixture of $[GdCp_3(OPPh_3)]$ and $OPPh_3$ was recovered from the filtrate. Attempted synthesis of $[YbCp_3(OPBu^n_3)]$ yielded $[\{YbCp_2(OPBu^n_3)\}_2O]$, the connectivity established by X-ray crystallography, and impure $[YbCp_3(OPBu^n_3)]$. Single crystal X-ray structure determination of $[YbCp_3(OPPh_3)]$ (monoclinic, space group $P2_1$, $a = 8.4187(7)$, $b = 17.019(11)$, $c = 9.450(7)$ Å, $\beta = 97.97(6)°$, $Z = 2$, $R = 0.043$ for 1576 observed data) showed the complex to contain formal ten coordinate ytterbium with distorted pseudo tetrahedral stereochemistry whilst the structure of $[NdCp_3(OPBu^n_3)]$ (trigonal, space group $P31/c$, $a = b = 12.973(4)$, $c = 9.657(6)$ Å, $Z = 2$, $R = 0.052$ for 602 observed data) showed ten coordinate neodymium with a distinctly trigonal pyramidal arrangement of oxygen and the centroids (Ct) of the Cp rings (Ct–Nd–Ct 119.8°). © 1998 Elsevier Science S.A. All rights reserved.

Keywords: Organolanthanoids; Cyclopentadienyl; Phosphine oxides; X-ray structure; Ytterbium; Neodymium

---

1. Introduction

Phosphine oxide complexes, mainly those of triphenylphosphine oxide are quite well known in inorganic lanthanoid chemistry [2] and have assisted in the crystallisation of highly reactive organoamidolanthanoids e.g. bis(trimethysilyl)amides [3,4] and 3,5-disubstituted pyrazolates [5,6]. Relatively few tertiary phosphine oxide organolanthanoid complexes are known [7–11] and all involve $OPPh_3$. In some cases the phosphine oxide was essential to the successful crystallisation of the organometallic moiety e.g. $[YbCp_2\{OPPh_2(C_5H_4)\}(OPPh_3)]\cdot THF$ (Cp, cyclopentadienyl and THF, tetrahydrofuran) [9] and *cis*- and *trans*-$[\{Sm(C_5Me_5)_2(OPPh_3)\}_2(\mu\text{-}OCH{=}CHO)]\cdot PhMe$ [7]. A notable feature of the organolanthanoid complexes is the strength of the Ln–O bond since Ln–$OPPh_3$ distances (allowing for differences in lanthanoid ionic radii [12]) vary from similar to Ln–OAr distances [13,14] to 0.15 Å shorter. Known phosphine oxide complexes of tris(Cp)lanthanoids are restricted to $[La(IND)_3(OPPh_3)]$ (IND, indenyl) [10] and some derivatives of $Ln(C_5H_4PPh_2)_3$ [11]. We now report syn-

---

* Corresponding author. Tel.: +61 3 99054568; fax: +61 3 99054597.

[1] Part XXII, see Ref. [1].

[2] Dedicated to my friend Professor Michael Bruce on the occasion of his 60th birthday in recognition of his distinctive and valuable contribution to organometallic chemistry.

PII S0022-328X(98)00456-2

Table 1
Phosphorus–oxygen stretching frequencies (cm^{-1})

Compound	ν(P=O)	Compound	ν(P=O)	Compound	ν(P=O)
[LaCp$_3$(OPPh$_3$)]	1157	[SmCp$_3$(OP(*o*-tolyl)$_3$)]	1148	[LaCp$_3$(OPBu$^n_3$)]	1135
[NdCp$_3$(OPPh$_3$)]	1161	[Nd(MeCp)$_3$(OPPh$_3$)]	1159	[NdCp$_3$(OPBu$^n_3$)]	1133
[SmCp$_3$(OPPh$_3$)]	1164	[Nd(MeCp)$_3$(OP(*o*-tolyl)$_3$)]	1151	[YbCp$_3$(OPBu$^n_3$)]	1139
'[GdCp$_3$(OPPh$_3$)]'	1165	OP(*o*-tolyl)$_3$	1185	OPBu$^n_3$	1155
[YbCp$_3$(OPPh$_3$)]	1168				
OPPh$_3$	1195				

theses of tertiary phosphine oxide (OPR$_3$; R = Ph, *o*-tolyl, or Bu^n) complexes of tris(Cp)- and tris(MeCp)-lanthanoids (MeCp, methylcyclopentadienyl), the X-ray crystal structures of [YbCp$_3$(OPPh$_3$)] and [NdCp$_3$(OPBu$^n_3$)], and the adventitious preparation of [{YbCp$_2$(OPBu$^n_3$)}$_2$O].

2. Results and discussion

The [LnCp$_3$(THF)] (Ln = La, Nd, Sm or Yb) reagents and [Nd(MeCp)$_3$(THF)] were prepared by redox transmetallation (Eq. (1)) [15–17], which has not previously been used to give the lanthanum complex.

$$\text{Ln} + 3\text{TlCp} \rightarrow \text{LnCp}_3 + 3\text{Tl}\downarrow \qquad (1)$$

Reaction of [LnCp$_3$(THF)] (Ln = La, Nd, Sm, or Yb) with OPPh$_3$ (mole ratio 1:1 or 1:2) in DME (DME, 1,2-dimethoxyethane) yielded the complexes [LnCp$_3$(OPPh$_3$)] (Eq. (2)).

$$\text{LnCp}_3(\text{THF}) + \text{OPPh}_3 \rightarrow [\text{LnCp}_3(\text{OPPh}_3)] + \text{THF} \qquad (2)$$

However, attempts to prepare the Gd complex from reaction of [GdCp$_3$(THF)] with OPPh$_3$ in THF or DME surprisingly crystallised unsolvated GdCp$_3$, whilst a mixture of [GdCp$_3$(OPPh$_3$)] and OPPh$_3$ was recovered from the filtrate from the reaction in THF. Treatment of unsolvated GdCp$_3$ with the phosphine oxide in toluene gave a mixture of GdCp$_3$ and [GdCp$_3$(OPPh$_3$)]. From analogous syntheses, [Nd(MeCp)$_3$(OPR$_3$)] (R = Ph or *o*-tolyl) and [SmCp$_3$(OP(*o*-tolyl)$_3$)], were prepared. The tributylphosphine oxide complexes [LnCp$_3$(OPBu$^n_3$)] (Ln = La, Nd) were similarly prepared by addition of the ligand to filtered transmetallation reaction mixtures. An attempt to prepare [YbCp$_3$(OPBu$^n_3$)] by this procedure gave on crystallisation a low yield of [{YbCp$_2$(OPBu$^n_3$)}$_2$O], the connectivity of which was established by an incomplete structure determination (see below), followed by the impure target complex, which was identified spectroscopically. The oxide is considered to be derived from a trace of adventitious water (Eq. (3)).

$$2[\text{YbCp}_3(\text{OPBu}^n_3)] + \text{H}_2\text{O} \rightarrow 2\text{CpH} + [\{\text{YbCp}_2(\text{OPBu}^n_3)\}_2\text{O}] \qquad (3)$$

The possibility that the oxide was formed from oxidation of some residual YbCp$_2$ (accompanying formation of YbCp$_3$ in Eq. (1)) by the phosphine oxide (Eq. (4))

$$2\text{YbCp}_2 + 3\text{OPBu}^n_3 \rightarrow [\{\text{YbCp}_2(\text{OPBu}^n_3)\}_2\text{O}] + \text{PBu}^n_3 \qquad (4)$$

was eliminated when treatment of YbCp$_2$ with tributylphosphine oxide did not lead to a colour change, in contrast to authentic oxidations of YbCp$_2$ to YbCp$_2$X complexes [18–20].

The formation of the complexes was readily evident from the expected [21,22] lowering of ν(P=O) of the phosphine oxide (Table 1) on coordination. The shift to higher energies with increasing atomic number for the OPPh$_3$ complexes is considered to be significant as the positions were reproducible to within 1 cm^{-1} with repeated spectra. A similar effect has previously been noted for [Ln(OPPh$_3$)$_2$(NO$_3$)$_3$]·S$_n$ (S = EtOH, $n = 1$; S = Me$_2$CO, $n = 2$) complexes [23] and more recently for [Ln(Ph$_2$pz)$_3$(OPPh$_3$)$_2$]·(DME)$_n$ (Ph$_2$pz, 3,5-diphenylpyrazolate) complexes [5,6]. The trend is unexpected at first sight, as both the mass effect and shorter Ln–O bonding with heavier (hence smaller) Ln elements could lead to lowering of ν(P=O) with increased atomic number. It has been explained by increased coupling of ν(Ln–O) and ν(P=O) as the Ln–O bond strength increases with decreasing Ln^{3+} radius [23]. For the tributylphosphine oxide complexes, ν(P=O) for Ln = Yb is at higher energies than for Ln = La or Nd, consistent with the trend, whilst ν(P=O) of [Nd(MeCp)$_3$(OPPh$_3$)] is close to the value for the corresponding unsubstituted Cp (Table 1).

Electron impact mass spectra of the phosphine oxide complexes did not show parent ions i.e. [LnCp$_3$(OPR$_3$)]$^+$. Typically, intense ions were observed for free OPR$_3$ and their associated fragments, and LnCp$_x^+$ (or Ln(MeCp)$_x^+$) ($x = 1$–3). However, the highest mass ions detected were generally weak phosphine oxide containing species such as LnCp$_2$(OPPh$_3$)$^+$ (Ln = La, Sm), Nd(MeCp)$_2$(OPR$_3$)$^+$ (R = Ph, *o*-tolyl) and LnCp$_2$(OPBu$^n_3$)$^+$ (Ln = La, Nd). Neutral donor:lanthanoid complexes often do not survive under electron impact mass spectral conditions, for example [LnCp$_3$(THF)] [15] or [{YbCp$_3$}$_2$(μ-pyrazine)] [24] gave only ions derived from dissociation of L including $LnCp_3^+$ and L^+. The detection of the lanthanoid–phosphine oxide species in the mass spectra presumably reflects the relatively strong $Ln–OPR_3$ bonding as indicated by the short Ln–O distances in the structures of $[YbCp_3(OPPh_3)]$ and $[NdCp_3(OPBu^n_3)]$ (see below).

Characteristic near infrared f → f transitions of Nd^{3+}, Sm^{3+} and Yb^{3+} were observed for solutions of $[LnCp_3(OPR_3)]$ in THF and these were not identical with those of the THF complexes [15,25]. Similarly, the LMCT band of $[YbCp_3(OPPh_3)]$ at 617 nm is shifted from that of $YbCp_3(THF)$ in THF (650 nm) [25]. Thus, significant phosphine oxide coordination is maintained in this medium. Further evidence was provided by the ^1H- and ^{31}P-NMR data obtained for d_8-THF solutions of the phosphine oxide complexes[3], in particular those of the paramagnetic Nd, Sm and Yb. Thus, for the $OPPh_3$ complexes, the *ortho*, *meta* and the *para* protons of the phenyl rings, observed as a single complex multiplet for diamagnetic $[LaCp_3(OPPh_3)]$, are split into distinct resonances in the ratio 6:6:3, respectively. The *ortho*-H resonances were the most affected and shifted by up to 37.4 ppm to higher frequency in the ytterbium case, clearly indicating a close proximity to the paramagnetic metal centre. Similar effects were observed in the ^1H-NMR spectra of the $OP(o\text{-tolyl})_3$ complexes and for the methylene protons of $OPBu^n$ in $[NdCp_3(OPBu^n_3)]$. The ^{31}P-NMR resonances of $[LaCp_3(OPR_3)]$ (R = Ph, Bu^n) in THF were both shifted to higher frequencies than for the free OPR_3 (R = Ph 25 ppm, Bu^n 45 ppm, in d_8-THF), consistent with coordination of the phosphine oxide to lanthanum. The paramagnetism of Nd, Sm and Yb resulted in widely varying positions of the respective ^{31}P-NMR resonances for these compounds.

The ^1H-NMR data for several of the paramagnetic complexes in the non-coordinating solvent d_8-toluene consistently showed increased broadening and magnitude of the paramagnetic shifts in comparison with the data obtained in THF. This suggests that in the latter solvent, the phosphine oxide undergoes partial displacement by THF (Eq. (5)).

$$[LnCp_3(OPR_3)] + THF \rightarrow [LnCp_3(THF)] + OPR_3 \qquad (5)$$

Generally, resonances for both free and coordinated phosphine oxide were not observed in the ^1H- and ^{31}P-NMR spectra, presumably due to rapid exchange of OPR_3 leading to time averaged resonances. Cooling of these solutions to 230 K did not sufficiently slow the exchange to resolve signals for the separate components. The only exception was in the room temperature (r.t.) ^{31}P-NMR spectrum of $[Nd(MeCp)_3(OP(o\text{-tolyl})_3)]$ which showed, in THF, two broad peaks of unequal intensity at 36 and 108 ppm, whilst in toluene, only one peak at 106 ppm. Since the lower frequency resonance corresponds to the free ligand value (36.1 ppm in THF), it is attributed to uncoordinated $OP(o\text{-tolyl})_3$. Thus the other resonances are assigned to $[Nd(MeCp)_3(OP(o\text{-tolyl})_3)]$. It is possible that, in this case, steric repulsion between the three Cp methyls and the three *o*-methyl substituents on the phenyl rings impedes the exchange between free and coordinated $OP(o\text{-tolyl})_3$, allowing both species to be observed on the ^{31}P-NMR time scale. Addition of excess (ca. 2:1) $OPPh_3$ to solutions of $[LnCp_3(OPPh_3)]$ in d_8-THF resulted in ^1H and ^{31}P spectra which more closely resemble those of uncoordinated phosphine oxide. This is as expected for a fast exchange system. A similar effect has been seen [26] in the ^{31}P-NMR spectrum of the diamagnetic $[Zn(OPBu_3)_4(ClO_4)_2]$ upon addition of $OPBu_3$. The ^1H-NMR spectrum of $[NdCp_3(OPBu^n_3)]$ in d_8-toluene indicated the presence of a significant amount of THF in the sample. The NMR spectrum was obtained for the bulk material, isolated by rapid precipitation from a THF/light petroleum mixture and contrasts the absence of THF in the structure (see below) of single crystals grown by slow diffusion of light petroluem into a THF solution of the complex. The retention of some lattice THF in the initial product may have resulted from the faster crystallisation rate and the single crystals may represent a slightly more energetically favoured structure.

The molecular structures of $[YbCp_3(OPPh_3)]$ and $[NdCp_3(OPBu^n_3)]$ were determined by single crystal X-ray diffraction and are shown in Figs. 1 and 2, respectively. The atomic coordinates are listed in Tables 2 and 3 and selected intramolecular geometries in Tables 4 and 5. $[YbCp_3(OPPh_3)]$ crystallised in the chiral space group $P2_1$ and consists of three η^5-Cp rings and the oxygen of the $OPPh_3$ bound to a formal ten coordinate Yb centre. Higher R values were obtained for the opposite chirality to that shown in Fig. 1 (see Section 3). $[NdCp_3(OPBu^n_3)]$ crystallised in the trigonal space group $P31/c$ with the Nd, O and P lying on a crystallographic 3-fold axis. The complex is similar in overall appearance to $[YbCp_3(OPPh_3)]$ with three η^5-Cp ligands and a coordinated phosphine oxide and there was no evidence of electron density which could be attributed to a THF of crystallisation (see above).

The centroids (Ct) of the Cp rings and the oxygen describe a distorted tetrahedron for the Yb complex, as evidenced by the larger angles between the centroids of the Cp rings and smaller O–Yb–Ct angles (Table 4). These values are typical of $[LnCp_3L]$ complexes (e.g.

---

[3] Inconsistencies in the relative intensities of OPR_3 and Cp proton resonances were observed in the spectra of $[LaCp_3(OPPh_3)]$, $[NdCp_3(OP(o\text{-tolyl})_3)]$ and $[Nd(MeCp)_3(OP(o\text{-tolyl})_3)]$ obtained in d_8-THF (see Section 3). Analytical data for the La complex confirmed the purity of the bulk material and hence the excess Ph integration may arise from slight decomposition of the NMR sample. For the Nd complexes, integration of the broad peaks was unreliable but spectra were obtained in d_8-toluene with satisfactory integrations.

L = THF ⟨Ct–Ln–Ct⟩ ca. 117°, ⟨Ct–Ln–O⟩ ca. 100° [27]) whereas [La{N(SiMe$_3$)$_2$}$_3$(OPPh$_3$)] is more closely tetrahedral (⟨N–Ln–N⟩ 112.8°, ⟨N–Ln–O⟩ 105.9°) [3]. For [NdCp$_3$(OPBu$^n_3$)], the distortion from tetrahedral is markedly greater (Table 5), such that the geometry can best be described as trigonal pyramidal. The oxygen atom of the OPBu$^n_3$ ligand lies in the apical position and the three Cp centroids define the basal triangular plane. The Nd atom and the centroids are < 0.1 Å from the least squares plane $0.0x + 0.0y + 9.657z = 1.8768$. Trigonal pyramidal coordination of a lanthanoid has been previously observed for [Yb(OC$_6$H$_2$-2,4,6-Bu$^t_3$)$_3$(THF)], where the THF lies in the apical position [13].

The Yb–C and Nd–C distances of [YbCp$_3$(OPPh$_3$)] (Table 4) and [NdCp$_3$(OPBu$^n_3$)] (Table 5), respectively, are representative of [LnCp$_3$L] complexes (e.g. L = THF [27]), after accounting for the differences in the lanthanoid ionic radii [12]. Distinctive features of the present structures are the 'effective oxygen radii' of the phosphine oxide ligands, 1.16 Å (Yb) and 1.14 Å (Nd), derived from subtraction of the appropriate Ln^{3+} ionic radius (Yb^{3+} 1.10 Å, Nd^{3+} 1.20 Å [12] extrapolated/interpolated for CN = 10) from the Ln–O distances (Tables 4 and 5). These values are significantly lower than the effective oxygen radii obtained for THF in [LnCp$_3$(THF)] (av. 1.34 Å [27]). The phosphine oxide has less steric bulk, compared to THF, in the vicinity of the donor atom[4] and hence the spear shaped nature of the O=PR$_3$ ligand may allow for a closer approach to the lanthanoid centre. Effective oxygen radii of similarly spear shaped carbonyl ligands in [LnCp$_3$L] (L = O=CR$_2$) complexes (e.g. [DyCp$_3$(OCPh$_2$)] 1.26 [29]; [LnCp$_3$(OC(NMe$_2$)$_2$)], Ln = Ce 1.21, Nd 1.24 [30];

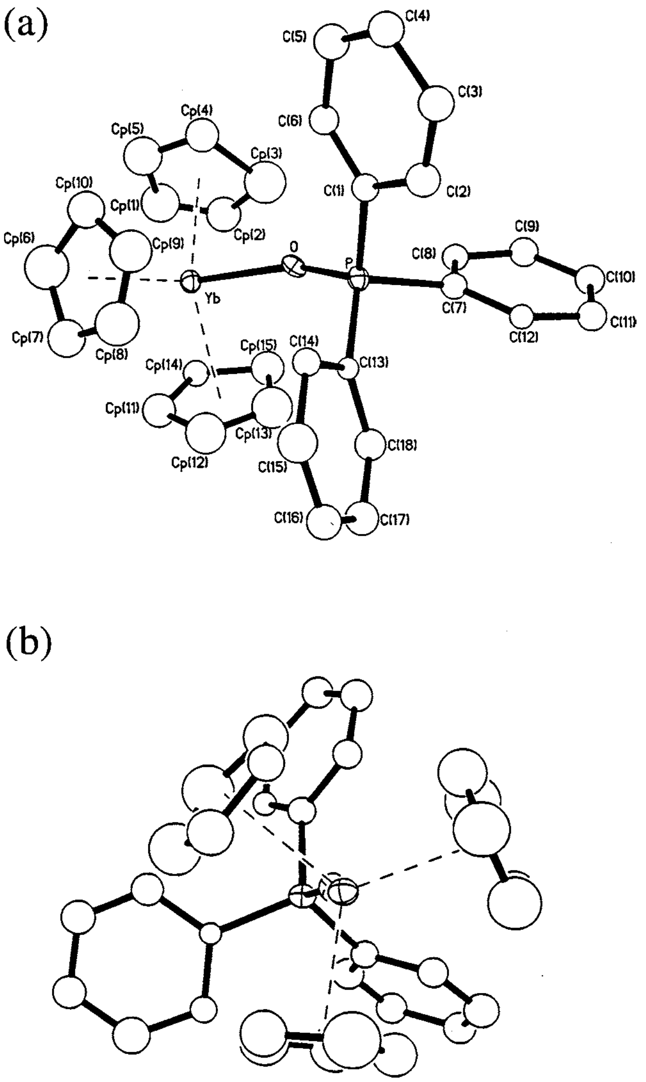

Fig. 1. (a) The molecular structure of [YbCp$_3$(OPPh$_3$)]; hydrogen atoms have been omitted. (b) Projection down the Yb–O axis.

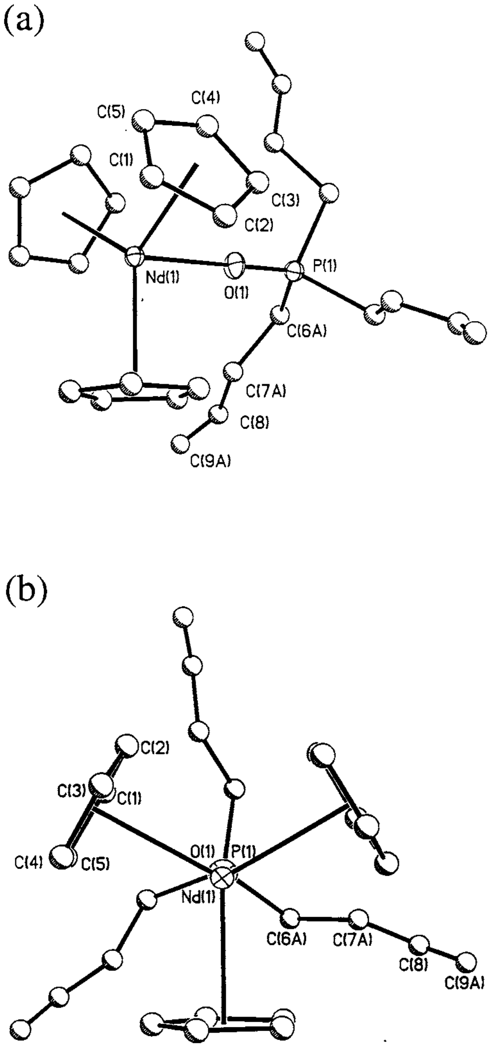

Fig. 2. (a) The molecular structure of [NdCp$_3$(OPBu$^n_3$)]; hydrogen atoms have been omitted. (b) Projection down the Nd–O–P axis.

---

[4] Overall, the bulk of OPPh$_3$ exceeds that of THF as indicated by their steric coordination numbers, 1.42 and 1.21, respectively [28].

[$PrCp_3$(n-butyl acetate)] 1.27 Å [31]) lie between those of THF and OPR_3. This suggests that electronic effects of the canonical form $O^-–P^+R_3$ may also contribute to the low effective oxygen radius in [$LnCp_3(OPR_3)$]. The Ln–O bonds are very much at the lower end of Ln–OPR_3 distances, which give effective oxygen radii of 1.10–1.22 Å in $OPPh_3$ complexes of lanthanoid cyclopentadienyls, indenyls [8–11] and pyrazolates [5,6], and 1.45–1.51 Å in $OPPh_3$ complexes of bis(trimethylsilyl)amidolanthanoids [3,4]. The effective oxygen radii do not correlate well with steric crowding. Thus although the largest sum of steric coordination numbers of ligands [28] (8.6) corresponds to a complex [$La\{N(SiMe_3)_2\}_2(PPh_2)(OPPh_3)_2$] [4] with a large oxygen radius (1.51), [$La(IND)_3(OPPh_3)$] [10] has a steric coordination number sum of 8.2 and one of the lowest oxygen radii (1.12), and [$La\{N(SiMe_3)_2\}_3(OPPh_3)$] [3] has a radius of 1.51 but a steric coordination number sum of only 7.9. For [$YbCp_3(OPPh_3)$], the sum of the ligand steric coordination numbers is 7.5. The P–O bond lengths of lanthanoid triphenylphosphine oxide complexes (range 1.47–1.54 Å) [2–11] also do not correlate with the effective oxygen radius and hence with the strength of the Ln–O bond. For [$YbCp_3(OPPh_3)$], the O–P distance (Table 4) lies in the previously observed range and is virtually unchanged from that of the free ligand (1.49 Å [32]) in contrast to the significant lowering of the ν(P=O) in the IR spectrum.

Table 2
Atomic coordinates ($\times 10^4$) and equivalent isotropic displacement coefficients ($Å^2 \times 10^3$) for [$YbCp_3(OPPh_3)$]

Atom	x	y	z	U(eq)
Yb	437(1)	2500	1349(1)	20(1)
P	−1182(6)	4098(3)	3506(5)	19(1)
O	−856(13)	3420(7)	2552(12)	22(4)
C(1)	−2351(21)	3752(11)	4918(19)	26(4)
C(2)	−2728(29)	4237(15)	6055(26)	36(6)
C(3)	−3675(24)	4010(13)	7042(22)	37(5)
C(4)	−4351(25)	3242(13)	6934(24)	39(5)
C(5)	−4006(26)	2765(12)	5811(23)	42(6)
C(6)	−3013(23)	3031(12)	4810(21)	31(5)
C(7)	−2394(22)	4856(11)	2595(20)	26(4)
C(8)	−3274(22)	4629(12)	1331(20)	28(4)
C(9)	−4400(25)	5148(13)	703(23)	36(5)
C(10)	−4545(24)	5901(13)	1239(21)	36(5)
C(11)	−3540(22)	6139(13)	2447(21)	33(5)
C(12)	−2508(21)	5588(11)	3097(19)	21(4)
C(13)	561(19)	4581(10)	4323(17)	16(4)
C(14)	1176(21)	4327(11)	5680(19)	24(4)
C(15)	2538(28)	4717(15)	6271(27)	47(6)
C(16)	3311(25)	5278(13)	5542(22)	37(5)
C(17)	2688(30)	5494(15)	4176(26)	38(7)
C(18)	1374(24)	5139(13)	3592(21)	34(5)
Cp(1)	−948(35)	1467(19)	−452(31)	71(8)
Cp(2)	−1658(29)	2091(16)	−792(28)	58(7)
Cp(3)	−2551(31)	2382(28)	248(28)	82(8)
Cp(4)	−2305(27)	1654(15)	1368(25)	49(6)
Cp(5)	−1310(34)	1179(18)	806(31)	66(7)
Cp(6)	2136(36)	1361(20)	2602(33)	78(9)
Cp(7)	3098(29)	2009(15)	2860(26)	54(6)
Cp(8)	2396(27)	2459(36)	3799(24)	69(6)
Cp(9)	1139(33)	2183(15)	4130(29)	63(7)
Cp(10)	866(28)	1486(16)	3552(24)	50(6)
Cp(11)	2884(30)	2884(15)	−162(25)	50(6)
Cp(12)	2783(36)	3531(18)	784(32)	71(8)
Cp(13)	1436(35)	3916(20)	330(32)	74(8)
Cp(14)	1617(23)	2877(12)	−1135(22)	31(5)
Cp(15)	611(30)	3531(15)	−837(26)	53(6)

U(eq) is defined as one third of the trace orthogonalised U_{ij} tensor.

Table 3
Atomic coordinates ($\times 10^4$) and equivalent isotropic displacement coefficients ($Å^2 \times 10^3$) for [$NdCp_3(OPBu^n_3)$]

Atom	x	y	z	U(eq)
Nd(1)	6667	3333	1852	24(1)
P(1)	6667	3333	−2135(8)	28(2)
O(1)	6667	3333	−576(23)	37(5)
C(1)	5039(27)	1214(30)	3152(22)	106(11)
C(2)	4464(23)	1256(26)	1921(29)	98(10)
C(3)	5069(29)	1110(33)	779(22)	141(24)
C(4)	6018(21)	977(23)	1305(28)	96(10)
C(5)	6000(24)	1041(31)	2772(27)	142(24)
C(6A)	7717(27)	4744(26)	−3039(40)	98(11)
C(7A)	7854(30)	5815(27)	−2202(31)	91(9)
C(9A)	8848(85)	7811(71)	−2099(87)	330(51)
C(8)	8487(28)	6995(22)	−2631(28)	73(7)

U(eq) is defined as one third of the trace orthogonalised U_{ij} tensor.

The Yb–O–P angle in [$YbCp_3(OPPh_3)$] (Table 4) compares well with those of other organolanthanoid phosphine oxide complexes e.g. [$YbCp_2(OPPh_3)_2$] (164(1) and 167(1)°) [8], *cis*- and *trans*-[$\{Sm(C_5Me_5)_2(OPPh_3)\}_2(\mu$-OCH=CHO)] (158.7(5)–

Table 4
Selected bond lengths (Å) and angles (°) for [$YbCp_3(OPPh_3)$]

Bond distances (Å)			
Yb–Cp(1)	2.66(3)	Yb–Cp(11)	2.67(3)
Yb–Cp(2)	2.68(3)	Yb–Cp(12)	2.72(3)
Yb–Cp(3)	2.66(3)	Yb–Cp(13)	2.75(3)
Yb–Cp(4)	2.72(2)	Yb–Cp(14)	2.69(2)
Yb–Cp(5)	2.72(3)	Yb–Cp(15)	2.72(3)
Yb–Cp(6)	2.64(3)	Yb–O	2.25(1)
Yb–Cp(7)	2.70(2)	O–P	1.50(1)
Yb–Cp(8)	2.75(2)	P–C(1)	1.81(2)
Yb–Cp(9)	2.71(3)	P–C(7)	1.82(2)
Yb–Cp(10)	2.71(2)	P–C(13)	1.81(2)
Bond angles (°)			
Ct(1)–Yb–Ct(2)	117(1)	O–Yb–Ct(1)	101.5(7)
Ct(1)–Yb–Ct(3)	117(1)	O–Yb–Ct(2)	97.6(8)
Ct(2)–Yb–Ct(3)	118(1)	O–Yb–Ct(3)	99.7(6)
Yb–O–P	161.8(7)	O–P–C(7)	112.3(8)
O–P–C(1)	108.9(8)	O–P–C(13)	115.4(7)
Torsion angles (°)			
O–P–C(1)–C(6)	−12.3	O–P–C(13)–C(18)	81.8
O–P–C(7)–C(8)	19.3		

Table 5
Selected bond lengths (Å) and angles (°) for [$NdCp_3(OPBu^n_3)$]

Bond distances (Å)			
Nd(1)–C(1)	2.79(3)	Nd(1)–O(1)	2.34(2)
Nd(1)–C(2)	2.78(3)	O(1)–P(1)	1.51(2)
Nd(1)–C(3)	2.78(4)	P(1)–C(6A)	1.86(3)
Nd(1)–C(4)	2.79(3)		
Nd(1)–C(5)	2.79(3)		
Bond angles (°)			
Ct(1)–Nd–Ct(1A)	119.8	Nd(1)–O(1)–P(1)	180.0
Ct(1)–Nd–O(1)	92.7	O(1)–P(1)–C(6A)	117(1)

168.8(7)°) [7] and [$Ln(C_5H_4PPh_2)_3(OPPh_3)$] (Ln = Nd, Er 164.9(5) and 166.4(3)°) [11]. When the structure of [$YbCp_3(OPPh_3)$] is viewed down the Yb–O axis (Fig. 1b) it can be seen that two of the phenyl ring planes, C(1)–C(6) and C(7)–C(12), are rotated slightly (Table 4) from the O–P axis, such that the *ortho* carbon atoms, C(6) and C(8), point towards the centre of a Ct–Yb–Ct angle. However, the remaining phenyl ring, C(13)–C(18), which lies closest to the Yb centre, has a much larger phenyl ring plane rotation (Table 4), such that it is nearly perpendicular to the O–P axis, and it also has the largest O–P–C(*ipso*) angle (Table 4). This arrangement presumably minimises steric repulsions between the Cp ligands and the Ph groups. In contrast to the Yb structure, [$NdCp_3(OPBu^n_3)$] has a linear coordination of the phosphine oxide as does also [$La(IND)_3(OPPh_3)$] [10]. Both the Nd (Fig. 2b) and La [10] structures display staggered arrangements of the three R groups and the Cp or IND ligands.

A single crystal of [$\{YbCp_2(OPBu^n_3)\}_2O$] was also examined by X-ray diffraction. The structure solution indicated disorder in the Bu^n groups and not all of the C atoms of these groups could be located. In addition the Cp rings exhibited poor refinement characteristics (see Section 3). Nevertheless, the basic structural connectivity was clearly evident and confirmed the identity of the complex. The results have been lodged with the Supplementary Data. Visual examination of the remaining crystals did not yield further specimens suitable for X-ray analysis.

3. Experimental

3.1. General remarks

All the lanthanoid complexes described are extremely air- and moisture-sensitive. Thus, all reactions and manipulations of these compounds were carried out under purified nitrogen or argon, using Schlenk-, vacuum line- and dry box-techniques. Analytical and spectroscopic methods and instrumentation were generally as described previously [1,5,6,11]. Solvents were dried and deoxygenated by refluxing over sodium/benzophenone and were distilled under nitrogen into storage flasks equipped with greaseless Teflon valves. Commercial OPR_3 (R = Ph, Bu^n) ligands were sublimed before use to ensure the compounds were anhydrous. OP(*o*-tolyl)$_3$ was prepared from P(*o*-tolyl)$_3$ (1.0 g, 3.3 mmol), which was dissolved in acetone, and a 30% w/v solution of H_2O_2 (0.40 ml, 4.0 mmol) added. The hygroscopic product was obtained by sublimation ($110°C/2 \times 10^{-2}$ mmHg) of the evaporated reaction mixture. M.p. (in air) 152–153°C (lit. 153°C for the hemi-hydrate [33]). IR ν(Nujol): 1185 ν(P=O) cm^{-1}. MS: *m/z* 320 [M^+]. Solid [$LnCp_3(THF)$] (Ln = Nd, Sm, or Yb) and [$Nd(C_5H_4Me)_3(THF)$] were prepared by the literature procedure [15–17]. [$LaCp_3(THF)$] was prepared by an analogous method from La (2.12 g, 15.3 mmol), TlCp (1.41 g, 5.1 mmol) and Hg (0.05 ml) in refluxing THF (50 ml) which gave 0.51 g (75%) of the product after filtration and evaporation of the solvent. ^1H-NMR (200 MHz, d_8-toluene): δ 5.94, s, Cp.

3.2. Syntheses

3.2.1. [Tris(cyclopentadienyl)(triphenylphosphine oxide)lanthanum(III)]

A sample of [$LaCp_3(THF)$] (0.52 g, 1.3 mmol) was dissolved in DME (40 ml) and the solution was filtered onto $OPPh_3$ (0.71 g, 2.6 mmol). The solvent was evaporated to 25 ml and the remaining solution was heated and then left to cool slowly to r.t. A colourless powder deposited which was collected by filtration and dried under vacuum. Yield 0.47g (60%). Anal. Found: C, 64.8; H, 5.2; La, 22.3%. $C_{33}H_{30}LaOP$ Calc.: C, 64.7; H, 4.9; La, 22.7%. IR ν(Nujol): 3053w, 1590w, 1484w, 1440m, 1312w, 1186w, 1158s, 1125m, 1091m, 1072w, 1012m, 998w, 774s, 750s, 694s, 668w, 617w, 539s, 514w, 474w cm^{-1}. ^1H-NMR (200 MHz, d_8-THF): δ 5.96, s, 15H, Cp; 7.75–7.98, m, 18H (expect 15H), $OPPh_3$. $^{31}P\{^1H\}$-NMR (121.50 MHz, THF): δ 37.9, s, $OPPh_3$. MS: *m/z* 547 [0.2, $LaCp_2(OPPh_3)^+$]; 334 [14, $LaCp_3^+$]; 277 [97, $(OPPh_3{-}H)^+$] and associated fragment ions; 269 [100, $LaCp_2^+$]; 204 [33, $LaCp^+$]; 66 [24, CpH^+].

3.2.2. [Tris(cyclopentadienyl)(triphenylphosphine oxide)neodymium(III)]

A sample of [$NdCp_3(THF)$] (0.62 g, 1.5 mmol) and $OPPh_3$ (0.43 g, 1.5 mmol) were dissolved in hot DME (35 ml). The resulting pale blue–purple solution was left to cool slowly to r.t. A pale blue precipitate deposited which was collected by filtration and dried under vacuum. Yield 0.63g (68%). Anal. Found: C, 64.0; H, 5.1; Nd, 23.3%. $C_{33}H_{30}NdOP$ Calc.: C, 64.2; H, 4.9; Nd, 23.4%. IR ν(Nujol): 1589w, 1441m, 1311w, 1186w, 1161s, 1124m, 1092m, 1072w, 1012m, 1000w, 780m, 756s, 724s, 694m, 539s cm^{-1}. ^1H-NMR (200 MHz, d_8-THF): δ −0.39, br s, 6H, *o*-H($OPPh_3$); 3.11, br s, 15H, Cp (coincident with a residual protonated THF peak); 7.40, br s, 6H, *m*-H(OPPh$_3$); 7.85, t, 3H, *p*-H(OPPh$_3$). ^{31}P{^{1}H}-NMR (121.50 MHz, THF): δ 92.8, br s, OPPh$_3$. MS: *m*/*z* 337 [2, NdCp$_3^+$]; 277 [100, (OPPh$_3$–H)$^+$] and associated fragment ions; 272 [12, NdCp$_2^+$]; 207 [7, NdCp$^+$]; 66 [70, CpH$^+$]. Vis–near IR [λ_{max} (ε)] (THF): 511 (4), 517 (2), 519 (2), 530 (8), 532 (7), 533 (7), 542 (2), 577 (27), 583 (27), 589 (88), 590 (60), 595 (117), 596 (84), 600 (21), 607 (12), 617 (3), 624 (3), 740 (7), 751 (5), 778 (1), 793 (6), 799 (7), 811 (4) nm (dm^3 mol^{-1} cm^{-1}).

3.2.3. [Tris(cyclopentadienyl)(triphenylphosphine oxide)samarium(III)]

A sample of [SmCp$_3$(THF)] (0.50 g, 1.2 mmol) was dissolved in DME (30 ml) and the solution was filtered directly onto OPPh$_3$ (0.39 g, 1.4 mmol). A colour change from orange to yellow was observed. The solvent was evaporated to 15 ml and the remaining solution was heated and then left to cool slowly to r.t. A bright yellow microcrystalline powder deposited which was collected by filtration and dried under vacuum. Yield 0.52g (69%). Anal. Found: C, 63.7; H, 5.0; Sm, 24.5%. C$_{33}$H$_{30}$OPSm Calc.: C, 63.5; H, 4.9; Sm, 24.1%. IR ν(Nujol): 3052w, 1590w, 1440m, 1312w, 1186w, 1164s, 1124m, 1093m, 1072w, 1013m, 998w, 782s, 758s, 725s, 694m, 668w, 671w, 539s, 514w cm^{-1}. ^{1}H-NMR (200 MHz, d$_8$-THF): δ 6.31, br s, 6H, *o*-H(OPPh$_3$); 7.78, br s, 6H, *m*-H(OPPh$_3$); 7.93, t, 3H, *p*-H(OPPh$_3$); 11.40, br s, 15H, Cp; (d$_8$-toluene) 5.62, br s, 6H, *o*-H(OPPh$_3$); 6.70, br s, 6H, *m*-H(OPPh$_3$); 6.84, t, 3H, *p*-H(OPPh$_3$); 11.36, br s, 15H, Cp. ^{31}P{^{1}H}-NMR (121.50 MHz, THF): δ 15.2, br s, OPPh$_3$. MS: *m*/*z* 560 [0.07, SmCp$_2$(OPPh$_3$)$^+$]; 495 [0.05 SmCp(OPPh$_3$)$^+$]; 430 (0.03, Sm(OPPh$_3$)$^+$]; 347 [5, SmCp$_3^+$]; 282 [17, SmCp$_2^+$]; 277 [100, (OPPh$_3$–H)$^+$] and associated fragment ions; 217 [15, SmCp$^+$]; 66 [45, CpH$^+$]. Vis–near IR [λ_{max} (ε)] (THF): 419 (176), 1064 (5), 1087 (8), 1104 (9), 1121 (2), 1221 (15), 1242 (28), 1269 (7), 1347 (11), 1382 (8) nm (dm^3 mol^{-1} cm^{-1}).

3.2.4. [Tris(cyclopentadienyl)(triphenylphosphine oxide)ytterbium(III)]

A sample of [YbCp$_3$(THF)] (0.50 g, 1.1 mmol) and OPPh$_3$ (0.34 g, 1.2 mmol) were dissolved in DME (40 ml) to give a red–green dichroic solution. [YbCp$_3$(OPPh$_3$)] was isolated by either of two methods. (i) The solvent was evaporated to 20 ml and the remaining solution was heated to reflux then left to cool slowly to r.t. Green single crystals formed. (ii) The solvent was evaporated to 5 ml and diethyl ether (35 ml) was added. A green precipitate deposited which was collected by filtration and dried under vacuum. Yield 0.52 g (71%). The two products were shown to be identical using IR and ^{1}H-NMR spectroscopy. Anal. Found: C, 61.3; H, 4.9%. C$_{33}$H$_{30}$OPYb Calc.: C, 61.3; H, 4.7%. IR ν(Nujol): 1590w, 1484w, 1439m, 1313w, 1168s, 1123m, 1094w, 1072w, 1013m, 998 sh, 789s, 766s, 724s, 695s, 617vw, 538s, 514w cm^{-1}. ^{1}H-NMR (200 MHz, d$_8$-THF): δ −35.6, vbr s, 15H, Cp; 13.4, br s, 3H, *p*-H(OPPh$_3$); 14.7, br s, 6H, *m*-H(OPPh$_3$); 45.2, br s, 6H, *o*-H(OPPh$_3$). ^{31}P{^{1}H}-NMR (121.50 MHz, THF): δ 155.9, br s, OPPh$_3$. MS: *m*/*z* 369 [1, YbCp$_3^+$]; 304 [4, YbCp$_2^+$]; 277 [100, (OPPh$_3$–H)$^+$] and associated fragment ions; 239 [6, YbCp$^+$]; 174 [3, Yb$^+$]; 66 [45, CpH$^+$]. Vis–near IR [λ_{max} (ε)] (THF): 381 (365), 617 (23), 894 (3), 939 (16), 955 (9), 985 (16), 1004 (12), 1017 (36) nm (dm^3 mol^{-1} cm^{-1}).

3.2.5. Attempted reaction between GdCp$_3$ and OPPh$_3$

A sample of [GdCp$_3$(THF)] (0.50 g, 1.2 mmol) was dissolved in hot THF (40 ml) and filtered onto OPPh$_3$ (0.36 g, 1.3 mmol). The solution was heated and then left to cool slowly to r.t. Long yellow needles deposited which were collected by filtration and dried under vacuum. An IR spectrum of the isolated solid only showed peaks attributable to Cp (i.e. GdCp$_3$). The IR spectrum of the evaporated filtrate showed a strong peak of uncoordinated OPPh$_3$ (1185 cm^{-1}) and a weaker peak attributable to [GdCp$_3$(OPPh$_3$)] (1165 cm^{-1}). This material was treated with hot toluene (50 ml), the solution was filtered and the filtrate was evaporated to 20 ml to give a yellow–beige precipitate. An IR spectrum showed this to be mainly GdCp$_3$. In a second reaction, freshly sublimed GdCp$_3$ (1.97 g, 5.59 mmol) and OPPh$_3$ (1.80 g, 6.50 mmol) were stirred in toluene (20 ml) for 12 h. The resulting suspension was heated and the deposited bright yellow solid was collected by filtration, washed with refluxing toluene and dried under vacuum. The filtrate was also evaporated to dryness. An IR spectrum of the yellow filtered solid showed it to be mainly GdCp$_3$ with a small amount of [GdCp$_3$(OPPh$_3$)] (ν(P=O) 1166 cm^{-1}), whilst an IR spectrum of the evaporated filtrate showed it to be predominantly OPPh$_3$. In a further attempt, [GdCp$_3$(THF)] (0.19 g, 0.45 mmol) was dissolved in hot DME (50 ml) and the solution was filtered onto OPPh$_3$ (0.13 g, 0.47 mmol). The solution was left to cool slowly to r.t. and deposited faint red needles which were shown by an IR spectrum to be GdCp$_3$.

3.2.6. [Tris(methylcyclopentadienyl)(triphenylphosphine oxide)neodymium(III)]

A sample of [Nd(MeCp)$_3$(THF)] (0.30 g, 0.66 mmol) and OPPh$_3$ (0.20 g, 0.70 mmol) were stirred in DME (30 ml) to give a blue solid and a blue solution. The blue solution was filtered and the solid remaining on the sinter was dissolved and recombined with the filtrate by refluxing the solvent continuously under reduced pressure in a closed Schlenk system. The solution was heated and left to cool slowly to r.t. Light blue–lilac crystals formed were collected by filtration and dried under vacuum. Yield 0.31 g (71%). Anal. Found: C, 65.1; H, 5.7; Nd, 21.8%. $C_{36}H_{36}NdOP$ Calc.: C, 65.5; H, 5.5; Nd, 21.9%. IR ν(Nujol and Fluorolube): 3056w, 2921w, 1590w, 1484w, 1438m, 1311w, 1159s, 1122m, 1093w, 1071w, 1047w, 1035w, 997w, 929w, 828m, 755s, 728s, 693m, 668w, 618w, 538s, 464w cm^{-1}. ^{1}H-NMR (300 MHz, d$_8$-THF): δ −0.74, vbr s, 4.5H (expect 6H), *o*-H($OPPh_3$); 1.00, br s, 9H, $C\mathit{H}_3Cp$; 5.30, vbr d, 12H, $MeC_5\mathit{H}_4$; 7.16, br s, 6H, *m*-H($OPPh_3$); 7.61, br s, 3H, *p*-H($OPPh_3$); (d$_8$-toluene): δ −2.30, vbr s, 6H, *o*-H($OPPh_3$); 0.09, br s, (expect 9H, overlapping TMS peak), $C\mathit{H}_3Cp$; 4.34, vbr d, 12H, $MeC_5\mathit{H}_4$; 5.39, vbr s, 6H, *m*-H($OPPh_3$); 5.81, vbr s, 3H, *p*-H($OPPh_3$). ^{31}P{^{1}H}-NMR (121.50 MHz, THF): δ 92.7, br s, $OPPh_3$. MS: *m*/*z* 580 [0.1, $Nd(MeCp)_2(OPPh_3)^+$]; 500 [0.06, $(Nd(MeCp)(OPPh_3)-H)^+$]; 379 [8, $Nd(MeCp)_3^+$]; 365 [1, $(Nd(MeCp)_3-CH_2)^+$]; 300 [39, $Nd(MeCp)_2^+$]; 286 [3, $(Nd(MeCp)_2-CH_2)^+$]; 277 [100, $(OPPh_3-H)^+$] and associated fragment ions; 220 [15, $(Nd(MeCp)-H)^+$]; 142 [5, Nd^+]; 79 [3, $MeCpH^+$]. Vis–near IR [λ_{max} (ε)] (THF): 532 (10), 534 (10), 579 (30), 586 (33), 591 (130), 593 (79), 598 (150), 601 (33), 607 (18), 742 (16), 755 (12), 793 (6), 800 (8), 804 (7), 812 (3), 867 (26), 885 (20) nm (dm^3 mol^{-1} cm^{-1}).

3.2.7. [Tris(cyclopentadienyl)(tris(2-methylphenyl) phosphine oxide)samarium(III)]

A sample of [$SmCp_3(THF)$] (0.50 g, 1.2 mmol) and OP(*o*-tolyl)$_3$ (0.42 g, 1.3 mmol) were stirred in DME (50 ml) to give a yellow solid and a yellow solution. The mixture was heated and left to cool slowly to r.t. The resulting solid was collected by filtration and dried under vacuum. Yield 0.45 g (56%). The residue from the evaporated filtrate was crystallised from DME (15 ml) and the material obtained was shown by IR to be identical to the first. Total yield 0.61 g (76%). Anal. Found: C, 64.6; H, 5.2; Sm, 22.2%. $C_{36}H_{36}OPSm$ Calc.: C, 64.9; H, 5.5; Sm, 22.6%. IR ν(Nujol): 3090w, 1592w, 1560w, 1285w, 1201w, 1162w, 1148s, 1116s, 1086w, 1066w, 1045w, 1016m, 959w, 884w, 809w, 783m, 766s, 740m, 718m, 691w, 569m, 530m, 490m, 464w cm^{-1}. ^{1}H-NMR (200 MHz, d$_8$-THF): δ 2.01, br s, ~9H (coincident with a residual protonated THF peak), $C\mathit{H}_3C_6H_4$; 6.15, vbr s, 3H, *o*-(H6)(OP(*o*-tolyl)$_3$); 7.38, t, 3H, *m*-(H5)(OP(*o*-tolyl)$_3$); 7.70, d, 3H, *m*-(H3)(OP(*o*-$MeC_6H_4)_3$); 7.80, t, 3H, *p*-H(OP(*o*-tolyl)$_3$); 11.82, vbr s, 15H, Cp. ^{31}P{^{1}H}-NMR (121.50 MHz, THF): δ 23.8, br s, $OPPh_3$. MS: *m*/*z* 347 [6, $SmCp_3^+$]; 319 [17, (OP(*o*-tolyl)$_3$−H)$^+$] and associated fragment ions; 282 [18, $SmCp_2^+$]; 217 [23, $SmCp^+$]; 152 [13, Sm^+]; 66 [15, CpH^+]. Vis–near IR [λ_{max} (ε)] (THF): 425 (192), 946 (2), 1049 (2), 1064 (4), 1075 (3), 1087 (7), 1105 (6), 1123 (2), 1206 (7), 1223 (15), 1242 (23), 1280 (7), 1323 (5), 1346 (7), 1417 (10), 1440 (8), 1471 (7), 1501 (13) nm (dm^3 mol^{-1} cm^{-1}).

3.2.8. [Tris(methylcyclopentadienyl) (tris(2-methylphenyl)phosphine oxide)neodymium(III)]

A sample of [$Nd(MeCp)_3(THF)$] (0.50 g, 1.1 mmol) and OP(*o*-tolyl)$_3$ (0.38 g, 1.2 mmol) were stirred in DME (30 ml) to give a blue solid and a blue solution. The blue solution was filtered and the solid remaining on the sinter was dissolved and recombined with the filtrate by refluxing the solvent continuously under reduced pressure in a closed Schlenk system. The solution was evaporated to 15 ml, heated and left to cool slowly to r.t. A pale blue powder deposited which was collected by filtration and dried under vacuum. Yield 0.36 g (47%). Anal. Found: C, 66.6; H, 6.3; Nd, 21.1%. $C_{39}H_{42}NdOP$ Calc.: C, 66.7; H, 6.0; Nd, 20.6%. IR ν(Nujol): 3061w, 1592w, 1567w, 1495w, 1287m, 1201w, 1164w, 1151s, 1138m, 1119s, 1088m, 1068w, 1031m, 958w, 935w, 883w, 853w, 818m, 808m, 761s, 754s, 718m, 691m, 617w, 568m, 530m, 490m, 462w cm^{-1}. ^{1}H-NMR (200 MHz, d$_8$-THF): δ −2.0, vbr s, 4H (expect 3H), *o*-(H6)(OP(*o*-tolyl)$_3$); 0.75 and 0.95 (overlapping broad peaks), 12H (expect 18H), $C\mathit{H}_3Cp$ and $C\mathit{H}_3C_6H_4$; 8.13 and 8.53 (overlapping broad peaks), 21H, $MeC_5\mathit{H}_4$, *m*-, *p*-H(OP(*o*-tolyl)$_3$); (d$_8$-toluene): δ −4.13, br s, 9H, $C\mathit{H}_3C_6H_4$; −3.23, br s, 3H, *o*-(H6)(OP(*o*-tolyl)$_3$); 0.18, br s, 9H, $C\mathit{H}_3Cp$; 3.35, vbr s, 6H, α-$MeC_5\mathit{H}_4$; 5.33, br s, 3H, *m*-(H5)(OP(*o*-tolyl)$_3$); 5.51, br s, 3H, *m*-(H3)(OP(*o*-tolyl)$_3$); 6.07, br s, 3H, *p*-(H4)(OP(*o*-tolyl)$_3$); 7.4 vbr (overlapping residual protonated toluene peaks) ~6H, β-$MeC_5\mathit{H}_4$. ^{31}P{^{1}H}-NMR (121.50 MHz, THF): δ 36.1, vbr, free OP(*o*-tolyl)$_3$; 107.5, vbr, coordinated OP(*o*-tolyl)$_3$ (ratio ca. 2:1); (d$_8$-toluene/toluene): δ 105.7, br s, coordinated OP(*o*-tolyl)$_3$; 109.2, impurity (ca. 20%). A similar impurity resonance was observed in the THF spectrum at ca. 114 ppm as a very broad peak slightly above the background noise. MS: *m*/*z* 622 [0.1, $Nd(MeCp)_2$(OP(*o*-tolyl)$_3$)$^+$]; 606 [0.05, ($Nd(MeCp)_2$(OP(*o*-tolyl)$_3$)−CH_2)$^+$]; 540 [0.06, (Nd(MeCp)(OP(*o*-tolyl)$_3$)−H)$^+$]; 379 [6, $Nd(MeCp)_3^+$]; 319 [20, (OP(*o*-tolyl)$_3$−H)$^+$] and associated fragment ions; 300 [30, $Nd(MeCp)_2^+$]; 286 [3, $(Nd(MeCp)_3-CH_2)^+$]; 220 [13, $(Nd(MeCp)-H)^+$]; 142 [6, Nd^+]; 79 [15, $MeCpH^+$].

3.2.9. [Tris(cyclopentadienyl)(tri-*n*-butylphosphine oxide)lanthanum(III)]

La metal (1.3 g, 9.3 mmol), TlCp (1.5 g, 5.6 mmol) and Hg (0.05 ml) were stirred in THF (40 ml) at 60°C for 5 days. The hot reaction mixture was filtered through a celite pad and the residue was washed with THF. A sample of $OPBu^n_3$ (0.82 g, 3.8 mmol) was added to the combined filtrate and washings and the resulting solution was concentrated to ca. 5 ml. Cooling of this solution in an ice/water mixture did not result in crystallisation. Addition of light petroleum precipitated an off white powder which was collected by filtration and dried under vacuum for 4 h. Yield 0.25 g (25%). Anal. Found: La, 24.2%. $C_{27}H_{42}LaOP$ Calc.: La, 25.2%. IR ν(Nujol): 3078w, 2724w, 1618w, 1314w, 1283vw, 1224w, 1135s, 1122m, 1090w, 1045vw, 1011m, 901w, 800w, 767m, 751vs cm^{-1}. ^{1}H-NMR (400 MHz, d$_8$-toluene): δ 0.90, t, 9H, $OP((CH_2)_3C\mathit{H}_3)_3$; 1.25, m, 18H, $OP((C\mathit{H}_2)_3CH_3)_3$; 6.14, s, 15H, Cp. $^{31}P\{^1H\}$-NMR (161.99 MHz, THF): δ 60.6, s, $OPBu^n_3$. MS: *m*/*z* 549 [6, $(M-3H)^+$]; 487 [9, $LaCp_2(OPBu^n_3)^+$]; 334 [22, $LaCp_3^+$]; 269 [100, $LaCp_2^+$]; 204 [25, $LaCp^+$]; 65 [27, Cp^+].

3.2.10. [Tris(cyclopentadienyl)(tri-n-butylphosphine oxide)neodymium(III)]·THF (1:1)

Nd metal (1.3 g, 9.3 mmol), TlCp (1.5 g, 5.6 mmol) and Hg (0.05 ml) were stirred in THF (40 ml) at 55°C for 5 days. The reaction mixture was filtered through a celite pad and the residue was washed with THF. A sample of $OPBu^n_3$ (0.40 g, 1.9 mmol) was added to the combined filtrate and washings. The resulting solution was stirred at r.t. for 1 h. Addition of light petroleum to the concentrated solution precipitated a blue powder which was collected by filtration and dried under vacuum. Yield 0.80 g (69%). Anal. Found: Nd, 21.9%. $C_{27}H_{42}NdOP\cdot(C_4H_8O)$ Calc.: Nd, 22.9%. IR ν(Nujol): 3089w, 2727w, 1600w, 1400w, 1313w, 1280w, 1224w, 1203w, 1133s, 1093m, 1044w, 1012s, 962w, 902w, 868vw, 842vw, 762s, 746vs cm^{-1}. ^{1}H-NMR (400 MHz, d$_8$-toluene): δ −9.35, br s, 6H, $OP(C\mathit{H}_2CH_2CH_2CH_3)_3$; −6.77, br s, 6H, $OP(CH_2C\mathit{H}_2CH_2CH_3)_3$; −1.29, br s, 6H, $OP(CH_2CH_2C\mathit{H}_2CH_3)_3$; 0.29, t, 9H, $OP((CH_2)_3C\mathit{H}_3)_3$; 1.52, m, 4H, β-H(THF); 2.05, br s, 15H, Cp; 3.66, m, 4H, α-H(THF) (some decomposition was evident by the presence of a peak at 6.27 ppm corresponding to the olefinic protons of free CpH). MS: *m*/*z* 492 [0.4, $NdCp_2(OPBu^n_3)^+$]; 429 [0.4, $NdCp_3(OPC_3H_7)^+$]; 369 [0.1, $NdCp(OPC_8H_{19})^+$]; 355, [0.7, $NdCp(OPC_7H_{17})^+$]; 337 [10, $NdCp_3^+$]; 272 [42, $NdCp_2^+$]; 218 [4, $(OPBu^n_3)^+$] and associated fragment ions. Single crystals suitable for crystallographic examination were grown from THF/petroleum spirit and had the composition $[NdCp_3(OPBu^n_3)]$.

3.2.11. [Tris(cyclopentadienyl)(tri-n-butylphosphine oxide)ytterbium(III)]

Yb metal (0.32 g, 1.9 mmol), TlCp (1.5 g, 5.6 mmol) and Hg (0.05 ml) were stirred in THF (40 ml) at 65°C for 24 h. The reaction mixture was filtered through a celite pad and the residue was washed with THF. A sample of $OPBu^n_3$ (0.40 g, 1.9 mmol) was added to the combined filtrate and washings. The resulting solution was stirred at r.t. for 1 h and then concentrated to 5 ml, heated and then left to cool slowly to r.t., which gave yellow–green single crystals of $[\{YbCp_2(OPBu^n_3)\}_2O]$ (identified by single crystal X-ray crystallography). To the remaining solution, light peteroleum (40 ml) was added resulting in precipitation of olive green $[YbCp_3(OPBu^n_3)]$ which was collected by filtration and dried under vacuum for 2 h. Yield 0.31 g (28%). Anal. Found: Yb, 30.3%. $C_{27}H_{42}OPYb$ Calc.: Yb, 29.5%. IR ν(Nujol): 1306w, 1278w, 1139s, 1117m, 1089w, 1044w, 1011m, 967w, 906w, 883vw, 753s, 722m cm^{-1}. $^{13}P\{^1H\}$-NMR (161.99 MHz, THF): δ 159.4, br s, $OPBu^n_3$; some impurities were present as indicated by weak resonances at ca. 50 ppm. MS: *m*/*z* 584 [28, $YbCp_3(OPC_{12}H_{24})^+$]; 519 [27, $YbCp_2(OPC_{12}H_{24})^+$]; 492 [10, $YbCp_2(OPC_{10}H_{21})^+$]; 457, [5, $YbCp(OPC_{12}H_{24})^+$]; 369 [5, $YbCp_3^+$]; 304 [11, $YbCp_2^+$]; 239 [20 $YbCp^+$]; 189 [28, $OPC_{10}H_{22}^+$]; 92 [100, $OPC_3H_9^+$].

3.3. X-ray structure determination

3.3.1. Crystal-refinement data

$C_{33}H_{30}OPYb$

$M = 646.6$; monoclinic; space group, $P2_1$ (C_2^2; no. 4) by successful refinement; $a = 8.418(7)$, $b = 17.019(11)$, $c = 9.450(7)$ Å; $\beta = 93.97(6)°$; $U = 1351(2)$ Å^3; $D_{calc.} = 1.59$ g cm^{-3}; $Z = 2$; $F(000) = 642$; μ(Mo–K$_\alpha$) = 35.3 cm^{-1}; specimen size 0.20 × 0.20 × 0.10 mm; crystal covered in heavy oil and cooled immediately to 150 K; no absorption correction; N (ω scan mode) = 1847, $N\sigma = 1576$; $R = 0.044$, $R_w = 0.056$ (opposite chirality 0.049 and 0.067, respectively); $n_v = 163$; $T = 150$ K. Mo–K$_\alpha$ (λ 0.71069 Å). Other specific procedural details: reflection weights, $\omega = [\sigma^2(F_o) + 0.0001760F_o^2]^-$; all calculations were performed with the Siemens SHELXTL PLUS software [34].

$C_{27}H_{42}NdOP$

$M = 557.8$; trigonal; space group, $P31/c$ (C_{3v}^4; no. 159) by successful refinement; $a = 12.973(4)$, $c = 9.657(6)$ Å; $U = 1407(1)$ Å^3; $D_{calc.} = 1.316$ g cm^{-3}; $Z = 2$; $F(000) = 574$; μ(Mo–K$_\alpha$) = 19.2 cm^{-1}; specimen size (ca.) 0.15 × 0.15 × 0.12 mm; crystal covered in heavy oil and cooled immediately to 173 K; no absorption correction; N (ω scan mode) = 662, $N\sigma = 602$; $R = 0.052$, $R_w = 0.139$ (all data); $n_v = 37$; $T = 173$ K. Mo–K$_\alpha$ (λ 0.71069 Å). Other specific procedural details: reflection weights, $\omega = [\sigma^2(F_o^2) + (0.0819{*}P)^2 + 9.34{*}P]^{-1}$ where $P = (\max(F_o^2, 0) + 2{*}F_c^2)/3$; all calculations were performed with the Siemens SHELXTL version 5.03 software [35].

$C_{44}H_{74}O_3P_2Yb$

$M = 1059.09$; monoclinic; space group, Cc (no. 9); $a = 18.474(7)$, $b = 35.174\ (12)$, $c = 16.737(7)$ Å; $\beta = 115.79(3)°$; $U = 9792(6)$ Å^3; $D_{calc.} = 1.437$ g cm^{-3}; $Z = 8$; $F(000) = 4256$; μ(Mo–K$_\alpha$) = 38.94 cm^{-1}; specimen size (ca.) 0.2 × 0.2 × 0.1 mm; crystal covered in heavy oil and cooled immediately to 173 K; no absorption correction; N (ω scan mode) = 6502, $N\sigma = 4723$; $R = 0.072$, $R_w = 0.081$; $n_v = 503$; $T = 173$ K. Mo–K$_\alpha$ (λ 0.71069 Å). Other specific procedural details: anisotropic thermal parameter forms were employed for the ytterbium atoms; H atoms were not included; not all of the C atoms of the butyl groups were able to be located and this was further hindered by their associated disorder; the Cp rings exhibited poor refinement characteristics and the maximum parameter shift in the final cycle was 11.79 × its estimated standard deviation; the max/min peaks on the final difference Fourier map were $2.46/-6.54$ e Å^{-3}; all calculations were performed with the teXsan crystallographic software package [36]; the results have been lodged with the Supplementary Data.

3.3.2. Structure determination

Unit cell parameters and intensity data sets were measured using a Siemens R3m/V four-circle diffractometer using graphite monochromatized Mo–K$_\alpha$ radiation at the specified temperatures within the limit $2\theta_{max} = 45°$. N independent reflections were obtained (see above), $N\sigma$ with $I > 3\sigma(I)$ (Yb) and $I > 2\sigma(I)$ (Nd) being considered 'observed' and used in the full matrix least squares refinement. Anisotropic thermal parameters were refined for atoms heavier than carbon; $(x, y, z, U_{iso})_H$ were constrained at the appropriate values for [YbCp$_3$(OPPh$_3$)]; $(x, y, z,$ group $U_{iso})_H$ refined for [NdCp$_3$(OPBu$^n_3$)]. Conventional R, R_w on $|F|$ (Yb) and F^2 (Nd) are quoted at convergence. Neutral atom complex scattering factors were employed [37]. The structures are displayed in Figs. 1 and 2, atomic coordinates are given in Tables 2 and 3 with selected bond distances and angles in Tables 4 and 5. Complete lists of bond distances and angles, thermal parameters and hydrogen atom coordinates are available from the Cambridge Crystallographic Data Centre (CCDC 101060).

Acknowledgements

We are grateful to the Australian Research council for financial support and for an Australian Postgraduate Research Awards (A. Philosof and P.A. White).

References

[1] G.B. Deacon, S.C. Harris, G. Meyer, D. Stellfeldt, D.L. Wilkinson, G. Zelesny, J. Organomet. Chem. 552 (1998) 159.
[2] F.A. Hart, in: G. Wilkinson, R.D. Gillard, J.A. McCleverty (Eds.), Comphrensive Coordination Chemistry, vol. 3, Pergamon, Oxford, UK, 1987, p. 1082.
[3] D.C. Bradley, J.S. Ghotra, F.A. Hart, M.B. Hursthouse, P.R. Raithby, J. Chem. Soc. Dalton Trans. (1977) 1166.
[4] H.C. Aspinall, S.R. Moore, A.K. Smith, J. Chem. Soc. Dalton Trans. (1992) 153.
[5] J.E. Cosgriff, G.B. Deacon, B.M. Gatehouse, Aust. J. Chem. 46 (1993) 1881.
[6] J.E. Cosgriff, G.B. Deacon, B.M. Gatehouse, H. Hemling, H. Schumann, Aust. J. Chem. 47 (1994) 1223.
[7] W.J. Evans, J.W. Grate, R.J. Doedens, J. Am. Chem. Soc. 107 (1985) 1671.
[8] G.B. Deacon, B.M. Gatehouse, P.A. White, Polyhedron 8 (1989) 1983.
[9] G.B. Deacon, B.M. Gatehouse, P.A. White, Aust. J. Chem. 45 (1992) 139.
[10] J. Guan, R.D. Fischer, J. Organomet. Chem. 532 (1997) 147.
[11] G.B. Deacon, C.M. Forsyth, A. Philosof, B.W. Skelton, A.H. White, Aust. J. Chem. 50 (1997) 959.
[12] R.D. Shannon, Acta Crystallogr. A32 (1976) 751.
[13] G.B. Deacon, T. Feng, S. Nickel, M.I. Ogden, A.H. White, Aust. J. Chem. 45 (1992) 671.
[14] G.B. Deacon, T. Feng, B.W. Skelton, A.H. White, Aust. J. Chem. 48 (1995) 741.
[15] G.B. Deacon, A.J. Koplick, T.D. Tuong, Aust. J. Chem. 37 (1984) 517.
[16] G.B. Deacon, G.N. Pain, T.D. Tuong, Inorg. Synth. 26 (1989) 17.
[17] G.B. Deacon, G.N. Pain, T.D. Tuong, in: W.A. Herrmann (Ed.), Synthetic Methods of Organometallic and Inorganic Chemistry, vol. 6, 3rd ed., Thieme, Stuttgart, 1996, p. 86.
[18] G.B. Deacon, S.H. Harris, G. Meyer, D. Stellfeldt, D.L. Wilkinson, G. Zelesny, J. Organomet. Chem. 525 (1996) 247.
[19] G.B. Deacon, D.L. Wilkinson, Aust. J. Chem. 42 (1989) 845.
[20] G.B. Deacon, D.L. Wilkinson, Inorg. Chim. Acta 142 (1988) 155.
[21] F.A. Cotton, R.D. Barnes, E. Bannister, J. Chem. Soc. (1960) 2199.
[22] G.B. Deacon, J.H.S. Green, Spectrochim. Acta 24A (1968) 845.
[23] D.R. Cousins, F.A. Hart, J. Inorg. Nucl. Chem. 29 (1967) 1745.
[24] E.C. Baker, K.N. Raymond, Inorg. Chem. 16 (1977) 2710.
[25] F. Calderazzo, R. Pappalardo, S. Losi, J. Inorg. Nucl. Chem. 28 (1966) 987.
[26] S.O. Grim, L.C. Satek, J. Coord. Chem. 6 (1976) 39.
[27] (a) F.T. Edelmann, in: E.W. Abel, F.G.A. Stone, G. Wilkinson (Eds.) Comprehensive Organometallic Chemistry II, vol. 4, Pergamon, Oxford, 1995, ch. 2, p. 11. (b) H. Schumann, J.-A. Meese-Marktscheffel, L. Esser, Chem. Rev. 95 (1995) 865 and references therein.
[28] J. Marçalo, A.P. De Matos, Polyhedron 8 (1989) 2431.
[29] X. Zhou, H. Ma, Z. Wu, X. You, Z. Xu, Y. Zhang, X. Huang, Acta Crystallogr. C52 (1996) 1875.
[30] A. Domingos, N. Marques, A.P. de Matos, M.G. Silva-Valenzuela, L.B. Zinner, Polyhedron 12 (1993) 2545.
[31] H. Schulz, H. Schultze, H. Reddmann, H.-D. Amberger, J. Organomet. Chem. 424 (1992) 132.
[32] For recent determinations of both monoclinic and orthorhombic forms see (a) C.P. Brock, W.B. Schweizer, J.D. Dunitz, J. Am. Chem. Soc. 107 (1985) 6964. (b) A.L. Spek, Acta Crystallogr. C43 (1987) 1233. (c) J.A. Thomas, T.A. Hamor, Acta Crystallogr. C49 (1993) 355.
[33] F.G. Mann, E.J. Chaplin, J. Chem. Soc. (1937) 527.
[34] G.M. Sheldrick, SHELX76 Program System, University of Cambridge, 1976.
[35] G.M. Sheldrick, SHELX93 Progam for Crystal Structure Determination, Universistät Göttingen, 1993.
[36] teXsan: Crystal Structure Analysis Package, Molecular Structure Corporation, 1985 and 1992.
[37] International Tables for X-ray Crystallography, vol. 4, Kynoch Press, Birmingham, UK (present distributor: D. Reidel, Dordrecht), 1974.